

Rapid Communications

The Rapid Communications section is intended for the accelerated publication of important new results. Since manuscripts submitted to this section are given priority treatment both in the editorial office and in production, authors should explain in their submittal letter why the work justifies this special handling. A Rapid Communication should be no longer than 3½ printed pages and must be accompanied by an abstract. Page proofs are sent to authors, but, because of the accelerated schedule, publication is not delayed for receipt of corrections unless requested by the author or noted by the editor.

Brillouin cross sections and localized phonons in CaF₂/Si heterostructures

J. M. Karanikas and R. Sooryakumar

Department of Physics, The Ohio State University, Columbus, Ohio 43210

Julia M. Phillips

AT&T Bell Laboratories, Murray Hill, New Jersey 07974

(Received 18 October 1988)

Up to seven acoustic surface modes have been observed by Brillouin scattering from CaF₂ films grown on Si(111). Striking variations of the intensities of the excitations with layer thickness are accounted for by interference between the different photon-coupling amplitudes. Together with the relative intensities of modes supported within each structure, these variations provide a critical test of the theory of surface Brillouin scattering from supported films. Wave-vector dependence of the amplitudes accounts for the different Brillouin line shapes observed in the dispersion of the elastic modes.

As the trend towards miniaturization continues in the semiconductor industry, physics in the vicinity of interfaces of submicron structures remains of great interest. Interfaces between elastically different media modify the surface acoustic phonons and often give rise to new localized modes. Observation of these modes and their dependence on structural parameters provides direct insight into the elastic properties of layered structures. Brillouin scattering is an excellent nondestructive means to detect these excitations and has recently been applied to supported¹ and unsupported² films as well as multilayer³ structures.

Simultaneously, theories of the Brillouin cross section based on two distinct mechanisms have been developed.⁴⁻⁸ The elasto-optic (EO) amplitude⁹ arises from the coupling of photons to the acoustic modulation of the dielectric constant and is largely effective in the bulk. Ripple scattering is induced by the dynamic corrugations confined near the interface; in a heterostructure the cross section will depend on the relative phase of the corresponding amplitudes at each interface.^{4,10} These amplitudes and the coherent interactions among them have been calculated leading to a general theory of the Brillouin cross sections from a supported film.⁸

The present work provides a systematic and critical test of the theory and establishes that the wave-vector dependence of the amplitudes can have a significant effect on the Brillouin spectra. Our measurements are on high-quality single-crystalline CaF₂ films grown epitaxially on Si. This system supports surface and interface ripple

scattering as well as EO scattering in the two media. By tuning the relative importance of the ripple contribution we show that both interfaces (air-CaF₂ and CaF₂-Si) have a strong influence on the intensity of the principal mode. Moreover, since up to six higher-order excitations are simultaneously observed, the spectra provide for a self-consistent evaluation of the theoretical cross sections. Interference among the various scattering amplitudes accounts for the negligible scattering from specific higher-order modes at certain film thicknesses. The evolution of the Brillouin line shapes with incident angle is accounted for by the wave-vector dependence of the scattering cross section.

CaF₂ was grown on Si(111) by molecular-beam epitaxy following the procedure described in Ref. 11. The film thickness h was determined by Rutherford backscattering. Brillouin spectra were measured at room temperature with 200 mW of p -polarized 5145 Å radiation. The backscattered photons were analyzed by a six-pass tandem Fabry-Pérot interferometer¹² with a finesse of 80. The throughput was checked between scans by measuring the intensity of the LA phonon of bulk CaF₂. The in-plane wave vector q_p of the detected phonons was parallel to $[\bar{1}10]$. The collection aperture was $f/1.4$ for measurements at an angle of incidence (θ) of 70°. For smaller θ 's it was reduced to $f/3.4$ to compensate for increased broadening.

Typical spectra from several films measured at $\theta=70^\circ$ are shown in Fig. 1(a) and display rich structure with increasing film thickness. The intensity of the lowest-lying

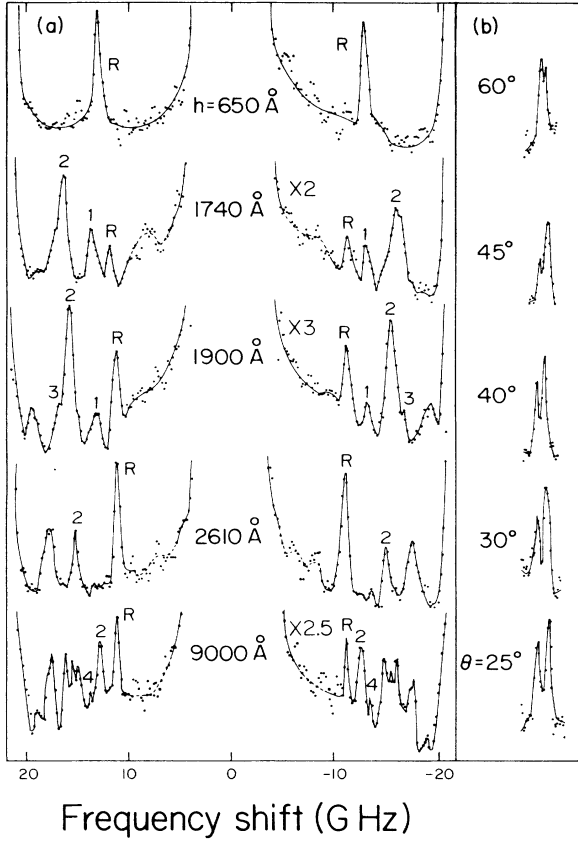


FIG. 1. (a) Measured Brillouin spectra of $\text{CaF}_2/\text{Si}(111)$ heterolayers for several insulator thicknesses h . The angle of incidence was 70° . (b) Evolution of a doublet of the principal mode R localized in the 650-Å film with angle of incidence.

inelastic peak labeled R , the principal (Rayleigh) mode, is strongly dependent on h (Fig. 2). It is sharp for all films studied. At larger frequency shifts, higher-order (Sezawa) modes, labeled 1, 2, 3 . . . , are observed consisting of partial waves whose displacement field propagates parallel to the surface but decays exponentially with distance into the substrate.^{13,14} In some instances ($h = 1740$ Å, 1900 Å), these excitations dominate the spectra. Under higher resolution, a splitting of the Brillouin peaks is observed and the relative intensities of the components of the resulting doublet are dependent on θ as shown in Fig. 1(b).

The general theory of Brillouin scattering from a thin film supported by a substrate has been previously developed.⁸ The total (EO plus ripple) cross section for backscattering in the sagittal plane for p and (p and s) polarizations of the incident (scattered) photons is given by

$$\frac{d^2\sigma}{d\Omega d\omega} \propto \cos\theta \sum_j |D(q_p, \Omega_j(q_p))|^2. \quad (1)$$

$D(q_p, \Omega_j(q_p))$, the scattering amplitude from the j th discrete mode of frequency Ω_j , can be expanded as the

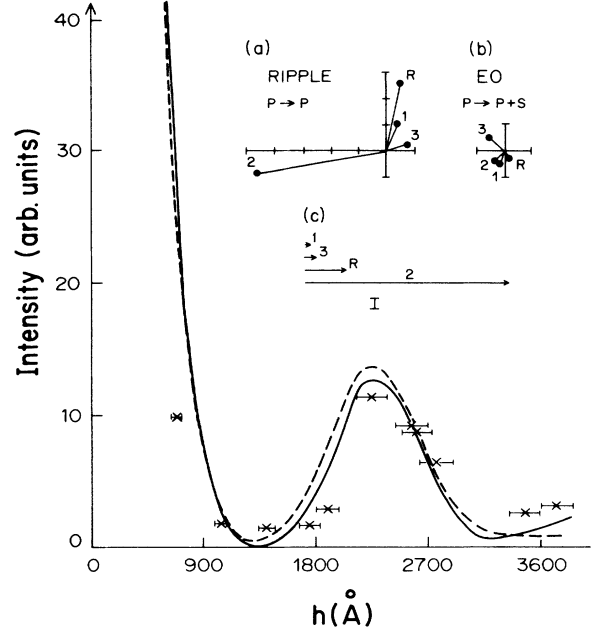


FIG. 2. Variation of the principal wave peak intensities with film thickness. The solid (dashed) curve is the calculated ripple plus elasto-optic (ripple only) contributions to the intensity. Both curves are normalized by the same single scaling factor. (a) and (b) are, respectively, the complex scattering amplitudes for the ripple and elasto-optic mechanisms of the lowest four guided waves for $h = 1900$ Å. (c) Calculated relative intensities of these four modes.

sum of the following EO and ripple (r) amplitudes.

$$D_{\text{EO}}^{p \rightarrow p} = [A(\delta\epsilon^f) + B(\delta\epsilon^s)],$$

$$D_{\text{EO}}^{p \rightarrow s} = [C(\delta\epsilon^f) + D(\delta\epsilon^s)],$$

$$D_r^{p \rightarrow p} = [E(W_z^f(h)) + F(W_z^s(0))].$$

Expressions for coefficients A – F have been derived and depend on many material parameters.⁸ $D_{\text{EO}}^{p \rightarrow p}$, $D_{\text{EO}}^{p \rightarrow s}$ are the EO contributions in the film (f) and substrate (s) according to their proportionality to $\delta\epsilon^f$ or to $\delta\epsilon^s$. The latter, $\delta\epsilon^{f,s}$, are the inhomogeneous parts of the dielectric tensor and depend on the strain tensor $\eta^{f,s}$: $\delta\epsilon_{\alpha\beta}^{f,s} = [K_{\alpha\beta\gamma\delta}^{f,s}][\eta_{\gamma\delta}^{f,s}]$. $K_{\alpha\beta\gamma\delta}^{f,s}$ are the elasto-optic coefficients in the two media and the values for Si were evaluated from Refs. 15 and 16. The following constants for CaF_2 were used:¹⁷ $\epsilon_0 = 2.062$, $k_{11} = 0.036$, $k_{12} = 0.56$, and $k_{44} = 0.086$.

$D_r^{p \rightarrow p}$ represents the ripple contributions from the air-CaF₂ interface at $z = h$ [$\propto W_z^f(h)$] and CaF₂-Si interface at $z = 0$ [$\propto W_z^s(0)$] where W_z is the normal component of the polarization vector of the acoustic waves. Hence, the overall ripple-induced scattering is dependent on the signs of the displacement fields at the free surface and Si interface.⁸ Symmetry of guided waves in the CaF₂ film requires $W_z(h)$ and $W_z(0)$ to have the same sign for the principal, second, fourth, and other even-ordered Sezawa modes. They are, however, directed oppositely for the

odd-ordered Sezawa waves.¹⁴ Coefficients E and F are sensitive to the relative phase $2q_0h$ between light diffracted by the dynamic gratings at the surface ($z=h$) and interface ($z=0$). Hence, for a given q_0 , [$q_0 = (\omega/c)(\epsilon_0^f - \sin^2\theta)^{1/2}$] the normal component of photon wave vector in the film, the Brillouin intensity derived from the ripple effect can be controlled by h . This tunability was exploited and led to the selection of the CaF_2 thicknesses used in this study.

The intensities of the principal mode (R) measured at $\theta=70^\circ$ from several films are shown in Fig. 2. The solid line is the calculated cross section based on Eq. (1). The measured intensity reveals an oscillatory behavior with h and displays minima around 1400 and 3500 Å. The agreement with theory is good except for the thinnest film $h=650$ Å. At this smallest thickness, however, the CaF_2 layer showed evidence¹⁸ of being strained, a fact that may account for the discrepancy. For comparison, we have also shown (as the dashed curve in Fig. 2) the cross section evaluated retaining only the ripple amplitudes. It is clear that $D_p^{p \rightarrow p}$ with contributions from both interfaces accounts for the major component of the Brillouin intensity in the CaF_2/Si structures. The weakness of the EO intensity can be traced to the small elasto-optic coefficients of CaF_2 and the higher-order effect that the dielectric modulations have near the surface where R is largely localized.

The dramatic drop in the measured intensity of the principal mode at 1400 and 3500 Å is controlled by the interference between ripple scattering at each interface, i.e., terms E and F . At these thicknesses $2q_0h \approx \pi, 3\pi$, and there is nearly perfect cancellation of the two ripple amplitudes. The subsequent increase of the intensity with h reflects the trend for these complex amplitudes to be more in phase. The ripple cross section does not recover its entire intensity of the low h values since $W_z(0)$ progressively gets smaller as h increases. The crossover of the solid and dashed curves of Fig. 2 that signals the absence of any EO contribution occurs around $h=800$ Å. It results when the EO amplitudes for the $p \rightarrow p$ and $p \rightarrow s$ scattering cancel. Subsequently, at thickness between about 800 and 3000 Å the curves of Fig. 2 show that the ripple and EO amplitudes destructively interfere.

The relative intensities of the higher-order modes provide another severe test of the theory of surface Brillouin scattering. It is noted from Fig. 1(a) that for the 1900 and 2610 Å films, the first higher-order localized phonon (1) is generally weak (and even absent from the 2610 Å film) in comparison to the neighboring Sezawa mode (2). To illustrate the importance of the various amplitudes that account for such relative strengths insets (a) and (b) to Fig. 2 show the complex scattering amplitudes for the four lowest modes at $h=1900$ Å. Figure 2(a) depicts the resultant amplitudes due to the ripple mechanism effective at both interfaces. Small amplitudes for peaks 1 and 3 arising from the corrugations are evident while mode 2 has, by far, the largest magnitude. This amplitude for the principal mode R is approximately twice that of mode 1. In comparison, Fig. 2(b) shows the small EO amplitudes. The vectors in the complex plane of Figs. 2(a) and 2(b) are oriented differently. For mode 1 they are almost out

of phase, leading to destructive interference between the ripple and EO contributions at this thickness. In contrast, the corresponding amplitudes for mode 2 augment a strong ripple effect. The relative intensities of R and modes 1, 2, and 3 based on the coherent coupling among the different amplitudes of Figs. 2(a) and 2(b) are illustrated in Fig. 2(c). Agreement with the measured spectra from $h=1900$ Å shown in Fig. 1(a) is good.

We now turn to the wave-vector dependence of the cross sections. Dispersion of localized modes $R, 1, 2, \dots$, is central to evaluating the elastic constants of thin films by Brillouin spectroscopy. Elastic continuum theory¹⁴ predicts that the sound velocities depend on the product $q_p h$. Hence, for a given film (i.e., fixed h) the dispersion measured in backscattering is controlled by θ ($q_p = 2k_i \sin\theta$, where k_i is the wave vector of the incident photon). Due to the analysis of photons within a finite solid angle, the wave-vector dependence of the scattering amplitudes can, as shown below, distort the Brillouin spectra. Hence, knowledge of the variation of the complex amplitudes with θ becomes especially significant.

To probe such effects θ was varied from 20° to 70° for the Brillouin measurements of each film. At small θ and increased resolution, the evolution of a splitting of the Brillouin peaks was observed. Further, the relative intensities of the components of the resulting doublet were dependent on θ . Spectra illustrating these features for the Stokes peak R from the $h=650$ Å film are shown in Fig. 1(b).

Two separate factors contribute to the splitting and the observed line shapes of the resulting doublet as θ is reduced. The splitting arises from the interception of photons backscattered towards the center of the collection aperture by the mirror directing the incident beam onto the sample. This results in minimal modifications to the Brillouin intensities measured at an aperture of $f/1.4$. The relative intensities of the doublet result from scattering cross sections of excitations characterized by a distribution of wave vectors that are analyzed within the finite collection solid angle [0.07 sr in Fig. 1(b)]. The cross section calculated from Eq. (1) for the $h=650$ Å sample has a broad maximum ($\sim 10^\circ$ wide) around 55° . The calculated intensity decreases steadily between $\theta=50^\circ$ and $\theta=20^\circ$.¹⁸ Hence, close to $\theta=60^\circ$, almost equal intensities are expected from the finite spread of wave vectors sampled in the collection optics. This is evident in the corresponding doublet in Fig. 1(b). At smaller θ , the scattering is more intense at wider angles (that lead to larger q_p) within the collection cone and accounts for the stronger high-energy component of the doublet when θ is below 50° . These different factors were further confirmed by the behavior when photons within known segments of the finite solid angle were intercepted. Hence, the *minimum* within the doublet identifies with wave vectors corresponding to perfect backscattering. Such line-shape analysis was considered and found to be crucial when components of the film elastic tensor and their dependence on thickness were evaluated from the dispersion.¹⁸

In summary, the Brillouin cross sections of several localized excitations in the supported CaF_2 films have revealed striking changes with layer thickness. The oscilla-

tory behavior of the principal and Sezawa mode intensities with h provide a critical test of the theory of surface Brillouin scattering. Further, the relative intensities of the higher-order modes supported within each film are well accounted for and provide additional insight into contributions from different scattering amplitudes. It is shown that the wave-vector dependence of the cross sections

influences the Brillouin line shapes significantly. These effects must be considered when elastic properties are derived from the dispersion of surface waves.

The work at The Ohio State University was supported by the National Science Foundation under Contract No. DMR 87-03980.

-
- ¹B. Hillebrands, S. Lee, G. I. Stegeman, H. Cheng, J. E. Potts, and F. Nizzoli, *Phys. Rev. Lett.* **60**, 832 (1988).
- ²M. Grimsditch, R. Bhadra, and I. K. Schuller, *Phys. Rev. Lett.* **58**, 1216 (1987).
- ³P. Baumgart, B. Hillebrands, R. Mock, G. Guntherodt, A. Boufelfel, and C. M. Falco, *Phys. Rev. B* **34**, 9004 (1986); A. Kueny, M. Grimsditch, K. Miyano, I. Banerjee, C. M. Falco, and I. K. Schuller, *Phys. Rev. Lett.* **48**, 166 (1982).
- ⁴R. Loudon, *Phys. Rev. Lett.* **40**, 581 (1978); *J. Phys. C* **11**, 2623 (1978).
- ⁵E. L. Albuquerque, R. Loudon, and D. R. Tilley, *J. Phys. C* **13**, 1775 (1980).
- ⁶N. L. Rowell and G. I. Stegeman, *Phys. Rev. B* **18**, 2598 (1978).
- ⁷K. R. Subbaswamy and A. A. Maradudin, *Phys. Rev. B* **18**, 4181 (1978).
- ⁸V. Bortolani, A. M. Marvin, F. Nizzoli, and G. Santoro, *J. Phys. C* **16**, 1757 (1983).
- ⁹A. Marvin, V. Bortolani, F. Nizzoli, and G. Santoro, *J. Phys. C* **13**, 1607 (1980).
- ¹⁰S. Mishra and R. Bray, *Phys. Rev. Lett.* **39**, 222 (1977); *Solid State Commun.* **32**, 621 (1979).
- ¹¹J. M. Phillips *et al.*, *J. Electrochem. Soc.* **133**, 224 (1986).
- ¹²J. R. Sandercock, in *Light Scattering in Solids III*, edited by M. Cardona and J. Guntherodt, *Topics in Applied Physics* Vol. 51 (Springer-Verlag, Berlin, 1982).
- ¹³B. A. Auld, in *Acoustic Fields and Waves in Solids* (Wiley, New York, 1973), Vols. 1 and 2.
- ¹⁴G. W. Farnell and E. Adler, in *Physical Acoustics, Vol. IX*, edited by W. P. Mason and R. N. Thurston (Academic, New York, 1972).
- ¹⁵M. Chandrasekhar, M. H. Grimsditch, and M. Cardona, *Phys. Rev. B* **18**, 4301 (1978).
- ¹⁶V. Bortolani, F. Nizzoli, G. Santoro, and J. R. Sandercock, *Phys. Rev. B* **25**, 3442 (1982).
- ¹⁷E. D. Schmidt and K. Vedam, *J. Phys. Chem. Solids* **27**, 1563 (1966); K. V. Rao and T. Narasimhamurthy, *ibid.* **31**, 876 (1969).
- ¹⁸J. M. Karanikas, R. Sooryakumar, and Julia M. Phillips, *J. Appl. Phys.* (to be published).